


Cite this: *RSC Adv.*, 2021, 11, 29537

# Iron-containing palygorskite clay as Fenton reagent for the catalytic degradation of phenol in water

Jie Xu,<sup>†</sup> Xuehai Yun,<sup>†</sup> Meng Li, Ye Tian, Xiaodong Lei<sup>ID</sup> and Fazhi Zhang<sup>ID\*</sup>

Heterogeneous Fenton systems have great application prospects in the catalytic degradation of organic wastewater; however, they are still not widely used in operation due to the difficulty of preparing catalysts in low yields and the high manufacturing cost. Herein, we report that a pristine iron-containing palygorskite clay can be used as a Fenton catalyst reagent without any retreatment. The composition, morphology, and structure of palygorskite clay, as well as the distribution and content of Fe element in palygorskite, were characterized via several physicochemical techniques. The degradation reaction of phenol in water was carried out as a probe reaction for the palygorskite Fenton reagent. The effects of the palygorskite content, pH value, and hydrogen peroxide concentration on the degradation efficiency of phenol were studied. Under optimum operating conditions, the chemical oxygen demand (COD) degradation efficiency of phenol reaches 94% with a reaction temperature of 20 °C and a reaction time of 15 min.

Received 14th July 2021  
Accepted 16th August 2021

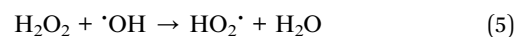
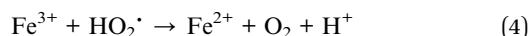
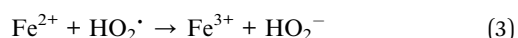
DOI: 10.1039/d1ra05416c

rsc.li/rsc-advances

## 1. Introduction

Water pollution is a critical issue affecting and constraining people's life and society's development.<sup>1,2</sup> The increased phenol pollution has become a major concern in environmental protection because they are highly toxic, carcinogenic and difficult to degrade.<sup>3,4</sup> Traditional research methods for phenol removal include biological treatment,<sup>5</sup> extraction,<sup>6</sup> and wet oxidation.<sup>7</sup> It was impossible to go into operation as all of these methods have limitations of high cost, low efficiency, secondary pollution and other factors. In recent years, advanced oxidation processes (AOPs) have been widely studied by scholars,<sup>4</sup> which generally includes Fenton oxidation,<sup>8,9</sup> ozone oxidation,<sup>10</sup> sonolysis oxidation,<sup>11</sup> super critical oxidation,<sup>12</sup> and photochemical oxidation.<sup>13</sup>

Compared with other methods of AOPs, the Fenton oxidation is easy to operate, and the process is relatively environmentally friendly. The mechanism of the Fenton oxidation is described as following:<sup>14,15</sup>



As mentioned above, in the presence of hydrogen peroxide ( $\text{H}_2\text{O}_2$ ), ( $\text{OH}$ ) was generated by the reaction between  $\text{Fe}^{2+}$  and  $\text{H}_2\text{O}_2$ , which can degrade the macromolecules into micro-molecules or mineralize the organic molecules into inorganic matters such as  $\text{CO}_2$  and  $\text{H}_2\text{O}$ . The clear disadvantage of the traditional homogeneous Fenton system was that it needed a higher concentration of  $\text{Fe}^{2+}$  in the solution. Some heterogeneous Fenton systems have been studied for improving the Fenton oxidation property. For example, Guo *et al.* synthesized a sulfur-doped  $\alpha\text{-Fe}_2\text{O}_3$  ( $\alpha\text{-Fe}_2\text{O}_3/\text{S}$ ) from ferrous sulfate and  $\text{Na}_2\text{S}_2\text{O}_3$  through a mixed hydrothermal calcination treatment for the degradation of acid orange 7 and phenol.<sup>16</sup> Xu *et al.* prepared a magnetic nano-scale  $\text{Fe}_3\text{O}_4/\text{CeO}_2$  composite via the impregnation method as a heterogeneous catalyst for the degradation of 4-chlorophenol.<sup>17</sup> In addition, some scholars found that the introduction of electricity, light and ultrasound can improve the Fenton oxidation efficiency, which led to the research on electron-Fenton,<sup>18,19</sup> photo-Fenton,<sup>20,21</sup> sono-Fenton,<sup>22,23</sup> sono-photo-Fenton,<sup>24</sup> sono-electron-Fenton,<sup>25</sup> and photo-electron-Fenton.<sup>26</sup> Although numerous methods were used for Fenton reagents to degrade organic wastewater, they are still difficult to be used in actual application because the methods are limited by the difficulty of preparing catalysts in low yields and high cost of catalyst preparation. Therefore, it is necessary to develop a simple heterogeneous Fenton system for the degradation of organics in water.

State Key Laboratory of Chemical Resource Engineering, Beijing University of Chemical Technology, Beijing, 100029, China. E-mail: zhangfz@mail.buct.edu.cn; Fax: +86-10-6442-5385; Tel: +86-10-6442-5105

<sup>†</sup> These authors contributed equally to this work.



Palygorskite clay, also known as attapulgite, is a kind of hydrous magnesium-rich silicate clay mineral with a chain-layered structure.<sup>27–30</sup> Its theoretical chemical formula is  $\text{Mg}_5\text{Si}_8\text{O}_{20}(\text{OH})_2(\text{OH}_2)_4 \cdot 4\text{H}_2\text{O}$ . Palygorskite is a fibrous porous crystal. The crystal structure unit layer is arranged by 8 Si–O tetrahedrons in a 2 : 1 type layer, where  $\text{Si}^{4+}$  can be replaced by  $\text{Fe}^{3+}$  or  $\text{Al}^{3+}$ , and  $\text{Mg}^{2+}$  by  $\text{Fe}^{2+}$ ,  $\text{Fe}^{3+}$  or  $\text{Al}^{3+}$ . The basic crystal unit forms a bundle with a chain structure, and the crystal is acicular, fibrous, or fibrous aggregate.<sup>29</sup> Palygorskite clay has been widely used in the fields of chemical industry, light industry, textile, building materials, environmental protection and pharmaceutical due to its specific fiber structure and excellent adsorption and decolorization properties.<sup>30</sup> In this study, we reported that a pristine iron-containing palygorskite clay can be used as a Fenton heterogeneous reagent without any retreatment. The composition, morphology, and structure of palygorskite clay, as well as the distribution and content of Fe element within it were studied *via* several physicochemical techniques. The effects of palygorskite content, pH value, and hydrogen peroxide concentration on the phenol degradation efficiency were also studied and the optimum operating conditions concluded were catalyst dosage of  $0.5 \text{ g L}^{-1}$ , initial pH = 3 and hydrogen peroxide dosage of  $30 \text{ mmol L}^{-1}$ . This study provides a catalyst material for improving the heterogeneous Fenton oxidation property.

## 2. Materials and methods

### 2.1 Materials

All the chemical reagents (phenol, hydrogen peroxide, sulfuric acid, sodium hydroxide, and hydrochloric acid) were of A.R. grade and used without further purification. The raw palygorskite clay, provided by Gansu Cuihua Technology Co., Ltd China, was passed through an 80-mesh sieve before use.

### 2.2 Characterization

X-ray diffraction (XRD) pattern was collected on a Shimadzu XRD-6000 X-ray powder diffractometer with Cu K $\alpha$  radiation ( $\lambda = 1.5406 \text{ \AA}$ ), and the scan rate was  $10^\circ \text{ min}^{-1}$ . Scanning electron microscopy (SEM) was carried out on Zeiss Supra 55. High-resolution transmission electron microscopy (HRTEM) uses Tecnai G2 produced by FEI. The determination of COD was based on a 5B-3C COD rapid analyzer produced by Lianhua Technology Co., Ltd China. The content of  $\text{Fe}^{3+}$  in the solution after the reaction was determined *via* ion chromatography (ICS-90A). The composition of palygorskite clay was tested on an X-ray fluorescence spectrometer (XRF-1800).

### 2.3 Catalytic experiment

Unless otherwise specified, all experiments were performed using 100 mL phenol ( $100 \text{ mg L}^{-1}$ ) with an appropriate pH value adjusted using  $0.5 \text{ mol L}^{-1} \text{ H}_2\text{SO}_4$  and  $1.0 \text{ mol L}^{-1} \text{ NaOH}$ . During the experiment,  $0.5 \text{ g L}^{-1}$  palygorskite was added to the phenol solution and magnetically stirred for 30 min (500 rpm) to establish an adsorption/desorption equilibrium at  $25^\circ \text{C}$ . Subsequently, different volumes of  $\text{H}_2\text{O}_2$  (30%) were added at

the required temperature. Finally, 5 mL of the mixed solution was taken out after a reaction time of 15 min and centrifuged at high speed (10 000 rpm, 3 min) to measure the COD and phenol concentration. The catalytic degradation efficiency is described as:  $[1 - (C_c/C_0)] \times 100$ , where  $C_0$  and  $C_c$  are the initial phenol COD value and the phenol COD value after the reaction, respectively. Effects of the palygorskite content, pH value, and hydrogen peroxide concentration on phenol degradation efficiency were also studied.

## 3. Results and discussion

### 3.1 Characterization of palygorskite clay

Fig. 1 shows the XRD pattern of raw palygorskite clay provided by Gansu Cuihua Technology Co., Ltd, China. There are numerous peaks stacked together. The highest peak was located at  $2\theta$   $26.6^\circ$ , which is characteristic of the quartz (101) crystal plane. In order to analyze the specific composition of palygorskite clay, we compared the impurity crystals with the JCPDS card. We can see that besides the palygorskite (JCPDS no. 21-0958), the raw attapulgite powder includes dolomite (JCPDS no. 36-0426), clinocllore (JCPDS no. 29-0701), muscovite-3T (JCPDS no. 07-0042), feldspar (JCPDS no. 70-1862), quartz (JCPDS no. 46-1045), calcite (JCPDS no. 47-1743), gypsum (JCPDS no. 21-0816),<sup>31</sup> and  $\text{Fe}_2\text{O}_3$  (JCPDS no. 40-1139).

SEM image of palygorskite with and without ultrasonic treatment of ethanol is shown in Fig. 2. It can be seen that various crystals interacted closely and superimposed on each other without ethanol ultrasound (Fig. 2a). However, the rod-shaped palygorskite crystals could not be distinguished from the other crystals. After palygorskite was ultrasonically dispersed in ethanol, we can clearly see the rod-shaped palygorskite (Fig. 2b). Palygorskite has a length of about  $0.4\text{--}3 \text{ }\mu\text{m}$ . In addition, we can see numerous flake impurity crystals after ultrasonic treatment of ethanol.

HRTEM was used to study the fine structure of the palygorskite sample (Fig. 3). The plane spacing between adjacent

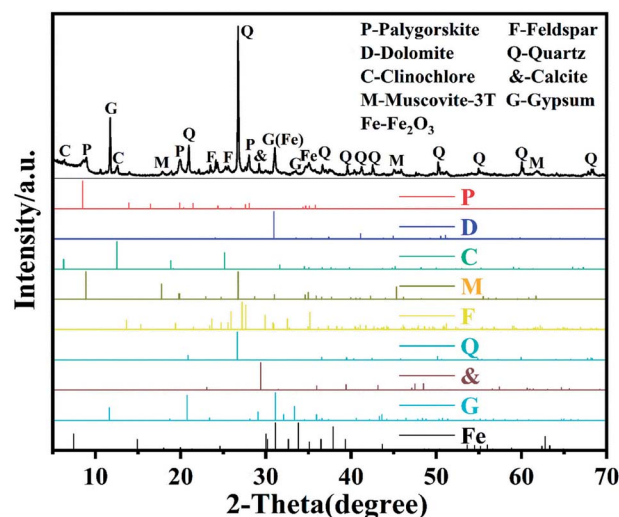


Fig. 1 XRD pattern of raw palygorskite clay.



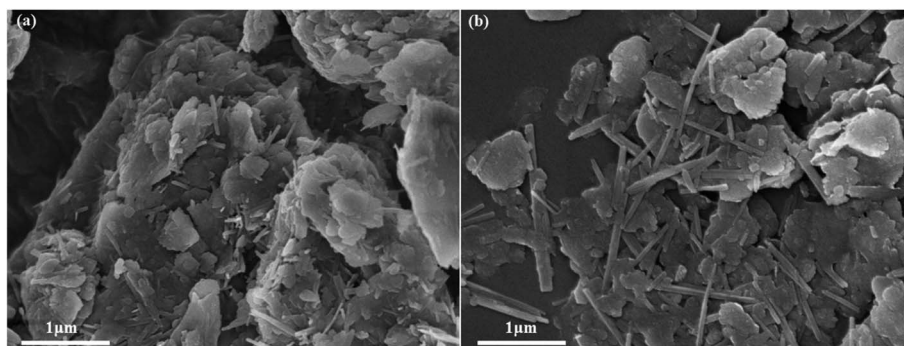


Fig. 2 SEM images of palygorskite without (a) and with ethanol ultrasound (b).

stripes on the edge of the palygorskite was measured to be 0.249 nm in HRTEM (Fig. 3a), exactly matching with the (110) (JCPDS no. 33-0664) crystal plane of  $\alpha$ -Fe<sub>2</sub>O<sub>3</sub>.<sup>32</sup> Linear scanning maps of Mg, Al, Si and Fe were obtained along the line shown in the HRTEM of the palygorskite sample (Fig. 3b and c), which shows that  $\alpha$ -Fe<sub>2</sub>O<sub>3</sub> is located at the edge of the palygorskite clay. An energy dispersive spectrometer was used to test the content of the elements of palygorskite clay (Fig. 3d). It was confirmed that palygorskite clay contained Mg, Al, Si and Fe, and their contents were determined to be 8.17%, 23.38%, 43.32% and 24.11%, respectively. In addition, the XRF test

shows the content of Fe<sub>2</sub>O<sub>3</sub> to be 9.9%. We suspected that Fe exists in the form of Fe<sub>2</sub>O<sub>3</sub> on the surface of palygorskite clay.

### 3.2 Catalytic activity of palygorskite clay

**3.2.1 Effect of palygorskite clay content.** The effect of the amount of palygorskite clay on the phenol degradation efficiency was investigated in the range of 0.01–2 g L<sup>−1</sup> of palygorskite (Fig. 4). As the content of palygorskite increases from 0.01 to 0.5 g L<sup>−1</sup>, the degradation efficiency of COD increases from 62% to 94%. With further increase in the quality of the palygorskite clay further increased, the COD degradation rate showed a decreasing trend, reaching a minimum of 60% at 2 g

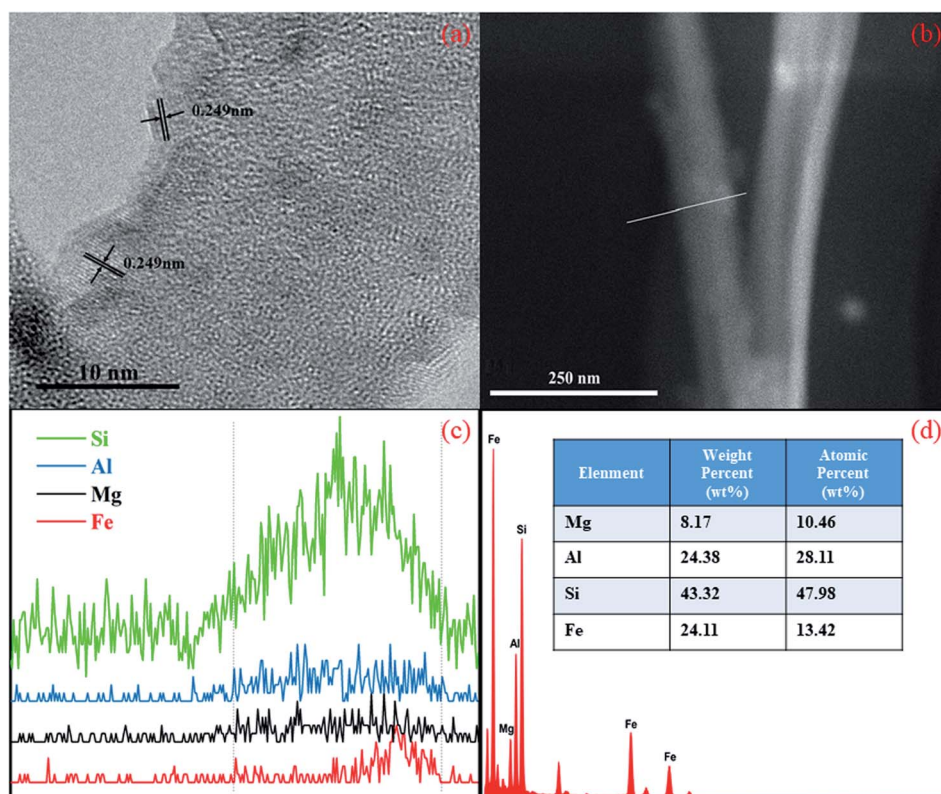


Fig. 3 (a) Enlarged HRTEM image of palygorskite clay. (b) HRTEM image of palygorskite clay. (c) Linear scanning maps of Mg, Al, Si and Fe along the line shown in the HRTEM of palygorskite clay. (d) EDS of palygorskite clay.





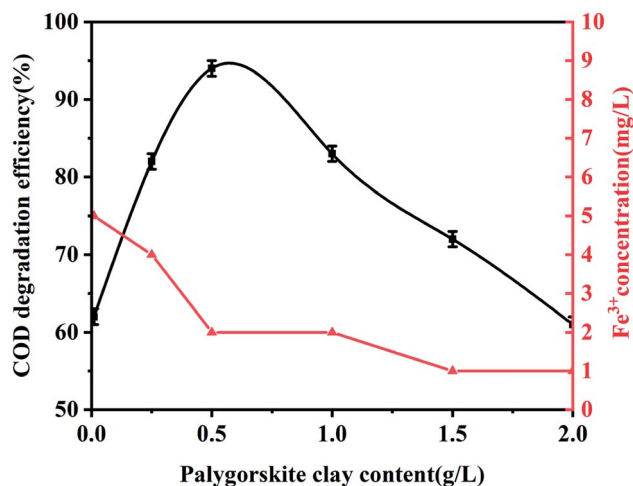


Fig. 4 Effect of palygorskite content on phenol degradation efficiency (other reaction conditions:  $\text{H}_2\text{O}_2$  concentration  $30 \text{ mmol L}^{-1}$ , initial pH value = 3, reaction temperature  $20^\circ\text{C}$ , and reaction time 15 min). The ordinate on the right represents the dissolution rate of  $\text{Fe}^{3+}$  in an aqueous solution. The results of the COD degradation efficiency presented in the graph are the average value calculated from three parallel experiments.

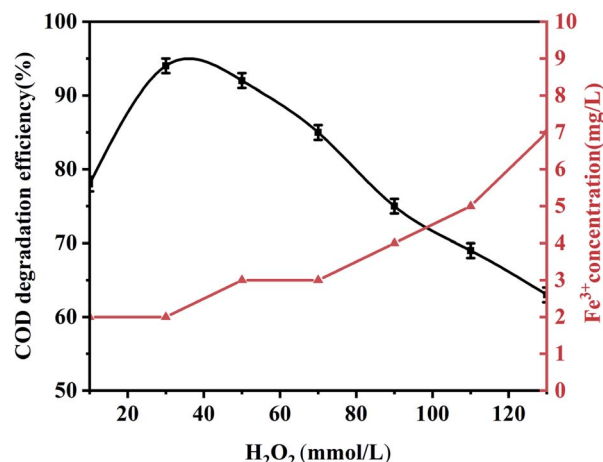


Fig. 5 Effect of  $\text{H}_2\text{O}_2$  concentration on phenol degradation efficiency (other reaction conditions: palygorskite content  $0.5 \text{ g L}^{-1}$ , initial pH value of 3, reaction temperature  $20^\circ\text{C}$ , and reaction time 15 min). The ordinate on the right represents the dissolution rate of  $\text{Fe}^{3+}$  in an aqueous solution. The results of the COD degradation efficiency presented in the graph are the average value calculated from three parallel experiments.

$\text{L}^{-1}$ . According to the mechanism of the Fenton system as described above,<sup>14,15</sup> the palygorskite clay content was smaller, and the  $\cdot\text{OH}$  radicals generated by the action between  $\text{H}_2\text{O}_2$  and  $\text{Fe}^{2+}$  were less, leading to low phenol degradation efficiency. If we added excessive palygorskite clay, a large amount of  $\cdot\text{OH}$  groups may rapidly be generated in the system. The excessive  $\cdot\text{OH}$  may accumulate and react with each other to offset the utilization of  $\cdot\text{OH}$  and reduce the degradation rate, thereby reducing the phenol degradation efficiency. We selected  $0.5 \text{ g L}^{-1}$  as the appropriate dose for subsequent experiments. Furthermore, the concentration of  $\text{Fe}^{3+}$  in the solution was measured after the reaction was carried out to evaluate the practicability of palygorskite in the degradation of organic wastewater. We can see that the  $\text{Fe}^{3+}$  concentration is lower than 5 ppm in the dosage range of  $0.01\text{--}2 \text{ g L}^{-1}$  of palygorskite.

In order to evaluate the effect of the Fe content of palygorskite on the phenol degradation efficiency, raw palygorskite was acidified using  $6 \text{ mol L}^{-1}$  hydrochloric acid (with a liquid-to-solid ratio of 10 : 1). The XRF test shows the content of  $\text{Fe}_2\text{O}_3$  was 3.5% for the acidified palygorskite. With the addition of  $0.5 \text{ g L}^{-1}$  palygorskite,  $30 \text{ mmol L}^{-1}$   $\text{H}_2\text{O}_2$  and with an initial pH value of 3, the phenol degradation efficiency was 34% for the above-acidified sample. The content of  $\text{Fe}_2\text{O}_3$  in the palygorskite clay was an important factor for degradation efficiency.

**3.2.2 Effect of  $\text{H}_2\text{O}_2$  concentration.** The effect of  $\text{H}_2\text{O}_2$  concentration on the degradation rate of phenol is shown in Fig. 5. When the concentration of  $\text{H}_2\text{O}_2$  increased from 10 to  $30 \text{ mmol L}^{-1}$ , the phenol degradation efficiency improved. However, when the  $\text{H}_2\text{O}_2$  increased to  $130 \text{ mmol L}^{-1}$ , the phenol degradation efficiency slowly decreased. When the concentration of  $\text{H}_2\text{O}_2$  is low, increasing  $\text{H}_2\text{O}_2$  will increase  $\cdot\text{OH}$ , resulting in an increase in the phenol degradation efficiency. Overdose of  $\text{H}_2\text{O}_2$  will lead to the rapid oxidation of  $\text{Fe}^{2+}$  to  $\text{Fe}^{3+}$ , thus

consuming  $\text{H}_2\text{O}_2$  and inhibiting the generation of  $\cdot\text{OH}$ .  $30 \text{ mmol L}^{-1}$  of  $\text{H}_2\text{O}_2$  will be used for the phenol degradation experiment. In addition, the  $\text{Fe}^{3+}$  content increases with the increase in the  $\text{H}_2\text{O}_2$  concentration, which may due to the reaction between  $\text{H}_2\text{O}_2$  and  $\text{Fe}^{2+}$  to form  $\text{Fe}^{3+}$ .

**3.2.3 Effect of pH value.** A relatively wide range of pH 1–9 was selected for testing the effect of pH on the Fenton reaction (Fig. 6). It was found that the phenol degradation efficiency gradually increased with the increase in pH from 1 to 3, reaching the maximum value of 94% when the pH was 3. As pH exceeds 3, the degradation efficiency gradually decreased.

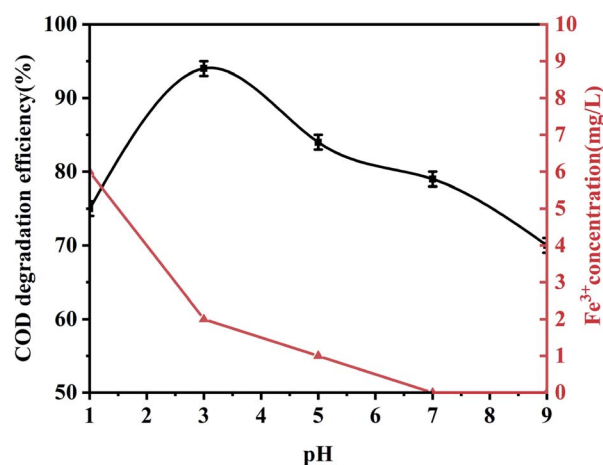


Fig. 6 Effect of initial pH value on phenol degradation efficiency (other reaction conditions: palygorskite content  $0.5 \text{ g L}^{-1}$ ,  $\text{H}_2\text{O}_2$  concentration  $30 \text{ mmol L}^{-1}$ , reaction temperature  $20^\circ\text{C}$ , and reaction time 15 min). The ordinate on the right represents the dissolution rate of  $\text{Fe}^{3+}$  in an aqueous solution. The results of the COD degradation efficiency presented in the graph are the average value calculated from three parallel experiments.



According to literature, the optimum pH of heterogeneous Fenton was 2.8.<sup>33,34</sup> If the pH value is lower than the optimum value,  $H^+$  in the system would be higher, which will break the conversion between different valence states of iron. If the pH value is higher, there would be too little  $H^+$  in the system, which will inhibit the formation of  $\cdot OH$  and influence degradation efficiency. Therefore, pH = 3 is selected as the optimum pH. In the experiment, the phenol degradation efficiency could be kept above 70% at a relatively broad pH of 1–9. In addition, we can see that  $Fe^{3+}$  decreases with the increase in pH and disappears in the solution after pH = 7. Based on the above experimental results, we found that the optimum operating conditions are the following: catalyst dosage of  $0.5\text{ g L}^{-1}$ , initial pH value of 3, and hydrogen peroxide dosage of  $30\text{ mmol L}^{-1}$ .

## 4. Conclusion

In summary, we reported that a pristine iron-containing palygorskite clay can be used as a heterogeneous Fenton reagent without any retreatment. Besides, palygorskite pristine powder sample includes impurity crystals such as gypsum, quartz, fluorophlogopite, and dolomite. We can clearly see the rod-shaped palygorskite after the powder sample was ultrasonically dispersed in ethanol. HRTEM and linear scanning map indicate that Fe exists in the form of  $Fe_2O_3$  on the surface of the palygorskite clay. The degradation of phenol in water was carried out as a probe reaction for the palygorskite Fenton reagent. The impact of several roles, such as palygorskite content,  $H_2O_2$  concentration, and pH value, on the phenol degradation efficiency has been studied. The optimum operating conditions utilized were palygorskite content of  $0.5\text{ g L}^{-1}$ , initial pH = 3, and hydrogen peroxide dosage of  $30\text{ mmol L}^{-1}$ . Under the optimum operating conditions, the COD degradation efficiency of phenol reached 94% within a reaction time of 15 min. The degradation ability of the palygorskite clay may be attributed to  $Fe_2O_3$  on the surface of palygorskite.

## Conflicts of interest

All authors declare that they have no conflict of interest.

## Acknowledgements

This work was supported by the National Natural Science Foundation of China (No. 21376019, 21676013) and Beijing Engineering Center for Hierarchical Catalysts.

## References

- 1 L. Schweitzer and J. Noblet, Chapter 3.6 – Water Contamination and Pollution, *Green Chem.*, 2018, 261.
- 2 Q. Wang and Z. Yang, Industrial water pollution, water environment treatment, and health risks in China, *Environ. Pollut.*, 2016, **218**, 358–365.
- 3 A. Haddadi and M. Shavandi, Biodegradation of phenol in hypersaline conditions by Halomonas sp. strain PH2-2 isolated from saline soil, *Int. Biodeter. Biodegr.*, 2013, **85**, 29–34.
- 4 A. Babuponnusami and K. Muthukumar, Advanced oxidation of phenol: a comparison between n Fenton, electro-Fenton, sono-electro-Fenton and photo-electro-Fenton processes, *Chem. Eng. J.*, 2012, **183**, 1–9.
- 5 H. H. P. Fang, D. W. Liang and T. Zhang, Anaerobic treatment of phenol in wastewater under thermophilic condition, *Water Res.*, 2006, **40**, 427–434.
- 6 W. Kujawski, A. Warszawski, W. Ratajczak, T. Porebski, W. Capafa and I. Ostrowska, Removal of phenol from wastewater by different separation techniques, *Desalination*, 2004, **163**, 287–296.
- 7 A. Santos, P. Yustos, S. Gomis, G. Ruiz and F. Garcia-Ochoa, Reaction network and kinetic modeling of wet oxidation of phenol catalyzed by activated carbon, *Chem. Eng. Sci.*, 2006, **61**, 2457–2567.
- 8 J. J. Pignatello, E. Oliveros and A. Mackay, Advanced Oxidation Processes for Organic Contaminant Destruction Based on the Fenton Reaction and Related Chemistry, *Crit. Rev. Env. Sci. Tec.*, 2006, **36**, 1–84.
- 9 H. L. Zheng, Y. X. Pan and X. Y. Xiang, Oxidation of acidic dye Eosin Y by the solar photo-Fenton processes, *J. Hazard. Mater.*, 2007, **141**, 457–464.
- 10 M. Sunder and D. C. Hempel, Oxidation of tri- and perchloroethene in aqueous solution with ozone and hydrogen peroxide in a tube reactor, *Water Res.*, 1997, **31**(1), 40.
- 11 Y. Segura, R. Molina, F. Martínez and J. A. Melero, Integrated heterogeneous sono-photo Fenton processes for the degradation of phenolic aqueous solutions, *Ultrason. Sonochem.*, 2009, **16**(3), 417–424.
- 12 I. V. Perez, Supercritical Water Oxidation of Phenol and 2,4-Dinitrophenol, *J. Supercritical. Fluids.*, 2004, **30**(1), 71–87.
- 13 A. M. Amat, A. F. Arques, F. Lopez and M. A. Miranda, Solar photo-catalysis to remove paper mill wastewater pollutants, *Sol. Energy.*, 2005, **79**(4), 393–401.
- 14 E. G. Garrido-Ramirez, B. K. Theng and M. L. Mora, Clays and oxide minerals as catalysts and nanocatalysts in Fenton-like reactions – a review, *Appl. Clay Sci.*, 2010, **47**(3–4), 182–192.
- 15 X. G. Shi, A. Tian, J. H. You, H. Yang, Y. Z. Wang and X. X. Xue, Degradation of organic dyes by a new heterogeneous Fenton reagent –  $Fe_2GeS_4$  nanoparticle, *J. Hazard. Mater.*, 2018, **353**, 182–189.
- 16 L. Q. Guo, F. Chen, X. Q. Fan, W. D. Cai and J. L. Zhang, S-doped  $\alpha\text{-Fe}_2O_3$  as a highly active heterogeneous Fenton-like catalyst towards the degradation of acid orange 7 and phenol, *Appl. Catal., B*, 2010, **96**(1–2), 162–168.
- 17 L. J. Xu and J. L. Wang, Magnetic Nanoscaled  $Fe_3O_4/CeO_2$  Composite as an Efficient Fenton-Like Heterogeneous Catalyst for Degradation of 4-Chlorophenol, *Environ. Sci. Technol.*, 2012, **46**(18), 10145–10153.
- 18 C. Flox, S. Ammar, C. Arias, E. Brillas, A. Vargas-Zavala and R. Abdelhedi, Electro-Fenton and photoelectro-Fenton degradation of indigo carmine in acidic aqueous medium, *Appl. Catal., B*, 2006, **67**(1–2), 93.



- 19 Y.-H. Huang, C.-C. Chen, G.-H. Huang and S. S. Chou, Comparison of a novel electro-Fenton method with Fenton's reagent in treating a highly contaminated wastewater, *Water Sci. Technol.*, 2001, **43**(2), 17–24.
- 20 S. Malato, J. Blanco, A. Vidal and C. Richter, Photocatalysis with solar energy at a pilot-plant scale: an overview, *Appl. Catal., B*, 2002, **37**(1), 1–15.
- 21 F. Martínez, G. Calleja, J. A. Melero and R. Molina, Heterogeneous photo-Fenton degradation of phenolic aqueous solutions over iron-containing SBA-15 catalyst, *Appl. Catal., B*, 2005, **60**(3–4), 181–190.
- 22 H. B. Ammar, Sono-Fenton process for metronidazole degradation in aqueous solution: effect of acoustic cavitation and peroxydisulfate anion, *Ultrason. Sonochem.*, 2016, **33**, 164–169.
- 23 R. Molina, F. Martínez, J. A. Melero, D. H. Bremner and A. G. Chakinala, Mineralization of phenol by a heterogeneous ultrasound/Fe-SBA-15/H<sub>2</sub>O<sub>2</sub> process: multivariate study by factorial design of experiments, *Appl. Catal., B*, 2006, **66**(3–4), 198–207.
- 24 Y. Segura, R. Molina, F. Martínez and J. A. Melero, Integrated heterogeneous sono-photo Fenton processes for the degradation of phenolic aqueous solutions, *Ultrason. Sonochem.*, 2009, **16**(3), 417–424.
- 25 M. E. Abdelsalam and P. R. Birkin, A study investigating the sonoelectrochemical degradation of an organic compound employing Fenton's reagent, *Phys. Chem. Chem. Phys.*, 2002, **4**(21), 5340–5345.
- 26 C. Flox, J. A. Garrido, R. M. Rodríguez, P. Cabot, F. Centellas, C. Arias and E. Brillas, Mineralization of herbicide mecoprop by photoelectro-Fenton with UVA and solar light, *Catal. Today*, 2007, **129**(1–2), 29–36.
- 27 Z. J. Zheng, J. G. Cheng, Y. H. Xia, M. Chen, J. Y. Zhou and K. Xu, Study on the Purification of Palygorskite clays, *Chin. Ceram. Soc.*, 2013, **32**(12), 2471–2475.
- 28 Z. Wang, W. Wei, Z. Z. Lin, Y. Kong, F. Wang and K. C. Yang, Research Progress on the Application of Palygorskite in Water Treatment, *J. Anhui Agric. Sci.*, 2012, **40**(16), 9048–9050.
- 29 Z. X. Yu, Z. Y. Lu, X. H. Zhao, C. X. Li, J. M. Pan and Y. S. Yan, Palygorskite Modification and Its Application in Environmental Water Treatment, *Bull. Chin. Ceram. Soc.*, 2010, **29**(6), 1367–1372.
- 30 P. Zhao, Y. Yao, F. Lin and C. X. Zhang, Application and Modification of Attapulgit, *Chem. Pro. Technol.*, 2006, **5**, 47–49.
- 31 J. Ren, L. L. Liu, L. Tao and C. W. Fu, Mineral Composition Analysis of Palygorskite from Gansu Area, *Bull. Chin. Ceram. Soc.*, 2013, **32**(11), 2362–2365.
- 32 M. H. Chen, J. L. Liu, D. L. Chao, J. Wang, J. H. Yin, J. Y. Lin, J. F. Hong and S. Z. Xiang, Porous  $\alpha$ -Fe<sub>2</sub>O<sub>3</sub> nanorods supported on carbon nanotubes-graphene foam as superior anode for lithium ion batteries, *Nano Energy*, 2014, **9**, 364–372.
- 33 N. N. Wang, T. Zheng, G. S. Zhang and P. Wang, A review on Fenton-like processes for organic wastewater treatment, *J. Environ. Chem. Eng.*, 2016, **4**(1), 762–787.
- 34 A. Babuponnusami and K. Muthukumar, A review on Fenton and improvements to the Fenton process for wastewater treatment, *J. Environ. Chem. Eng.*, 2014, **2**(1), 557–572.

